

Branching ratio study of $ZH \rightarrow q\bar{q}c\bar{c}/q\bar{q}b\bar{b}$

Hiroaki Ono¹ *

1 - Nippon Dental University School of Life Dentistry at Niigata
1-8 Hamaura-cho chuo-ku Niigata, Niigata - Japan

Precise measurement of the Higgs boson properties is an important issue of the International Linear Collider (ILC) experiment to verify the particles mass generation mechanism that the coupling strength between the Higgs boson and the fermions or vector bosons are proportional to the mass of each particle. Thus the measurement of the branching ratio of the Higgs boson an important issue to understand the mass of each particle. In this analysis, measurement accuracy of the Higgs boson branching ratio in the $ZH \rightarrow q\bar{q}H$ hadronic decay mode was studied with the cut-based analysis in Higgs mass of $M_H = 120$ GeV at the center-of-mass energy of $\sqrt{s} = 250$ GeV with the ILD detector model. From the analysis, we estimate the measurement accuracy of the relative Higgs boson branching ratio of $BR(H \rightarrow c\bar{c})$ to $BR(H \rightarrow b\bar{b})$ as 13.68%.

1 Introduction

International Linear Collider (ILC) [1] is a future e^+e^- collider experiment for the precise measurement and the validation of the Standard Model (SM) physics, especially for the measurement of the Higgs boson property, even the discovery of the Higgs boson will be realized in Large Hadron Collider (LHC) experiment. In the SM, light Higgs boson mass (M_H) is predicted the range of $M_H \geq 114.4$ GeV from the study in Large Electron Positron Collider (LEP II) [2] and recently Tevatron experiments exclude the Higgs mass range around $160 \leq M_H \leq 170$ GeV with the 95% confidence level [3]. From these results, Higgs mass is indicated to be light ($M_H \leq 140$ GeV) and in this region, Higgs mainly decays to $b\bar{b}$ pair which forms multi-jet final state, as shown in Fig. 1. Since hadron collider experiments have large QCD multi-jet backgrounds, the measurement of the light mass Higgs will not prefer in terms of the signal to noise ratio, ILC experiment has an advantage for precise measurement of light Higgs boson with large signal yield of multi-jet final state in lower background environment. Therefore, precise measurement of the light mass Higgs ($M_H \leq 140$ GeV) will be a primary target of the ILC experiment. At the lower center-of-mass energy (\sqrt{s}) range around the production threshold, as shown in Fig 2, SM Higgs boson is mainly produced through the Higgs-strahlung (ZH) process, which associated with the Z boson as shown in Fig. 3.

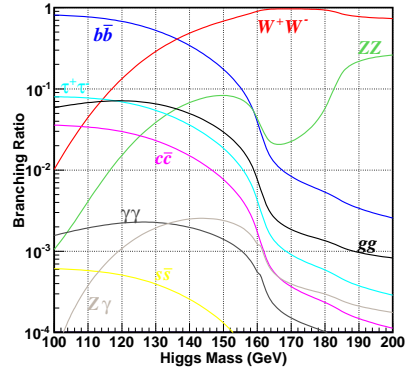


Figure 1: Branching fraction of the Higgs boson decay at the lower mass range ($100 \leq M_H \leq 200$ GeV).

*TEL:+81-25-267-1500 (537), MAIL: ono@ngt.ndu.ac.jp

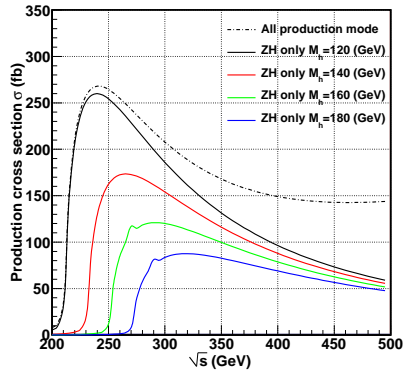


Figure 2: Production cross section of the Higgs with \sqrt{s}

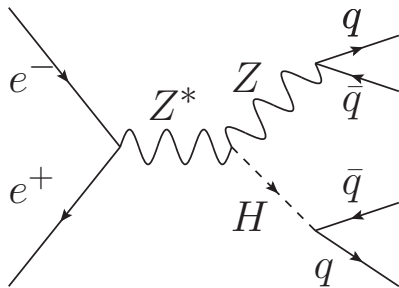


Figure 3: Higgs boson production via Higgsstrahlung (ZH) process.

For full detector simulation study, we use the ILD detector model based Monte Carlo (MC) full simulation package called Mokka, which is based on the MC simulation package Geant4 [4]. Generated MC hits are reconstructed and smeared in the reconstruction package called MarineReco which includes the PFA package called PandoraPFA [5]. Reconstructed hits are skimmed and saved in the ILC common data format called LCIO. For the event analysis, we use the useful analysis package library called Anlib and each analysis procedure is handled through JSF [7] based on Root [6]. In this analysis, we assume the center-of-mass energy around the ZH production threshold of $\sqrt{s} = 250$ GeV and the light Higgs mass of $M_H = 120$ GeV. Each data sample is scaled to the integrated luminosity of $\mathcal{L} = 250 \text{ fb}^{-1}$ and the beam

The largest production cross-section via ZH mode is obtained around the center-of-mass energy (\sqrt{s}) at the ZH production threshold region as shown in Fig. 2 (a). Since the Z boson mainly decays to $q\bar{q}$ pair, the largest Higgs boson production cross-section via ZH process is obtained through the $ZH \rightarrow q\bar{q}H$ process. Therefore, we study the Higgs boson property with the largest production cross-section process of $ZH \rightarrow q\bar{q}H$. Since Higgs boson mainly decays to $b\bar{b}$ pair at the Higgs mass below 140 GeV region as shown in Fig. 2 (b), the final state of the $ZH \rightarrow q\bar{q}H$ process forms the four-jet. In ILC experiment, two detector concepts, ILD and SiD submit their Letter of Intent (LOI) and validated by ILC Detector Advisory Group (IDAG). In order to achieve the best jet energy resolution in multi-jet environment, ILD adopt the Particle Flow Algorithm (PFA) suited detector design, which has fine-segmented calorimeter with strong magnetic field. In this analysis, we study the measurement accuracy of the branching ratio of Higgs boson with the full detector simulation for $ZH \rightarrow q\bar{q}H$ hadronic mode with the ILD detector model.

2 Analysis tools and MC samples

Table 1: Signal and background data samples.

Signal and Bkg	DST data samples
Higgs sample	$q\bar{q}H, \nu\bar{\nu}H, \ell\ell H$
SM background	$q\bar{q}q\bar{q}, \nu\ell q\bar{q}, \nu\bar{\nu}q\bar{q}, q\bar{q}, \ell\ell\ell, gg$

polarization to $P(e^+, e^-) = (+30\%, -80\%)$. The main backgrounds for ZH hadronic decay mode are considered as following processes: $ZH \rightarrow Z^*/\gamma \rightarrow q\bar{q}$, $e^+e^- \rightarrow WW/ZZ \rightarrow qq'q''q'''$ or $q\bar{q}q'\bar{q}'$, $\ell\ell q\bar{q}$, $\nu\bar{\nu}q\bar{q}$, $e^+e^- \rightarrow WW \rightarrow \nu\ell qq'$ and $e^+e^- \rightarrow ZZ \rightarrow \ell\ell\ell\ell$.

3 Event reconstruction

Since the final state of the $ZH \rightarrow q\bar{q}H$ mode forms four-jet, after the PandoraPFA clustering, forced four-jet clustering based on Durham jet-clustering algorithm has applied. In order to select the best jet pair combination from the four-jet, $d = (M_{12} - M_Z)^2 + (M_{34} - M_H)^2$ value is evaluated, where M_{12} is a Z candidate di-jet mass, M_{34} is a Higgs candidate di-jet mass, $M_{Z/H}$ are Z and Higgs boson masses. From the four-jet, minimum d value jets combination is selected as best Z and H candidates. In order to improve the background reduction from WW/ZZ with mass distribution, kinematic fitting is applied with following constraints after the jet pairing; $\sum E_i - E_{CM} = 0$, $\sum \vec{P}_i = 0$, $|M_{12} - M_{34}| = |M_Z - M_H|$ (di-jet mass difference consistent with Z and H mass difference), where E_i and \vec{P}_i are i -th jet energy and momentum which is sorted by energy, respectively.

After the jet pair combination and kinematic fitting, event selections are applied. For the ZH hadronic decay mode sample ($ZH \rightarrow q\bar{q}H$) selection from the pre-mixed sample of $ZH \rightarrow q\bar{q}/\nu\bar{\nu}/\ell\ell H$, following signal classification is applied: (0). Visible energy cut : $E_{vis} > 170$ GeV and no high momentum tracks ($P_{lepton} > 15$ GeV), After the classification, we apply the following selection criteria. In order to select the four jet reconstructed events, we require the number of charged tracks in each jet above four ($N_{charged} > 4$) and logarithm of the jet reconstruction Y -value threshold from three to four jet (Y_{34}) should be $-\log Y_{34} > 2.7$. After that, thrust, thrust angle ($\cos\theta_{thrust}$) and jets angle ($\theta_{H,Z}$) cuts are required to suppress the ZZ background from the difference of sphericity of final state jet shape. Finally we require the consistency of mass of the reconstructed jets pair after the kinematic fit that Z candidate jets pair should be consistent with M_Z and the other pair should be consistent with M_H . For the reduction of hard photons and ISR photons, finally highest photon energy cut is applied. Table. 2 shows the background reduction summary after the selections.

4 Branching ratio measurement

Branching ratio (BR) of Higgs boson is related to the mass of the fermions and gauge bosons. After the background reduction, we evaluate the measurement accuracy of the branching

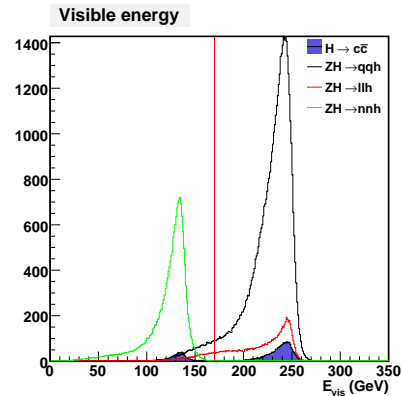


Figure 4: Visible energy distribution to select the $Z \rightarrow q\bar{q}$ hadronic mode from pre-mixed sample.

Table 2: Background reduction summary and its efficiency.

Selection criteria	$H \rightarrow c\bar{c}$	$H \rightarrow b\bar{b}$	Higgs Bkg	SM Bkg
Before the classification	2914	53480	23447	53333000
After the classification	1693	29075	9198	20528900
$N_{charged} > 4$	1238	22204	5721	3323060
$-\log(Y_{34}) > 2.7$	1218	21869	5694	2635920
$thrust < 0.95$	1217	21858	5693	2584510
$ \cos\theta_{thrust} < 0.96$	1157	20831	5427	2295690
$105^\circ < \theta_H < 165^\circ$	1080	19393	4941	1908300
$70^\circ < \theta_Z < 160^\circ$	1028	18490	4705	1776150
$110 < M_{H_{fit}} < 140$ GeV	982	17666	4411	1209100
$80 < M_{Z_{fit}} < 110$ GeV	982	17665	4409	1206570
$E_\gamma < 20$ GeV	895	16288	4063	1036990
Efficiency after classification	52.9% (ε_{cc})	56.0% (ε_{bb})	44.2%	5.0%

ratios (BR). In this analysis, we evaluate the relative branching ratios of $H \rightarrow c\bar{c}$ to $H \rightarrow b\bar{b}$: $\frac{BR(H \rightarrow c\bar{c})}{BR(H \rightarrow b\bar{b})}$. In order to evaluate the measurement accuracy of BR , we apply the flavor-likeness template fitting [9] after the all event selections. For each flavor, neural-net training is performed using $Z \rightarrow q\bar{q}$ Z -pole ($\sqrt{s} = 91.2$ GeV) samples in LCFIVertex package. Here, bc -likeness is a c -likeness trained only with $Z \rightarrow b\bar{b}$ background. Each flavor-likeness for di-jet is defined as: x -likeness = $\frac{x_1x_2}{x_1x_2 + (1-x_1)(1-x_2)}$, where $x_{1,2}$ are the neural-net trained output for b , c and bc flavor in each jet from the vertexing package of LCFIVertex [8] in ilcsoft. The analysis procedure of the template fitting is as following: (1). Prepare the b , c and bc three dimensional flavor-likeness template samples for $H \rightarrow b\bar{b}$, $c\bar{c}$, $others$ and SM Bkg decay modes; (2). Apply the Toy-MC template fitting test to evaluate the r_{bb} , r_{cc} , r_{others} and r_{bkg} , where r_{bb} , r_{cc} are the number of entry ratios of $H \rightarrow b\bar{b}$, $c\bar{c}$ after the selection cuts to the entry predicted from SM Higgs branching ratios, and r_{others} is a ratio of another Higgs decay modes which is described as $r_{others} = 1 - r_{bb} - r_{cc}$, and r_{bkg} is a normalized factor for the entries of SM background. (3). Estimate the relative branching fraction of $BR(H \rightarrow b\bar{b})/BR(H \rightarrow c\bar{c})$. In order to evaluate the fractions of Higgs decay mode in each sample, template fitting is applied with minimizing following χ^2 value:

$$\chi^2 = \sum_{i=1}^{n_b} \sum_{j=1}^{n_c} \sum_{k=1}^{n_{bc}} \frac{\left(N_{ijk}^{data} - \sum_{s=bb,cc,others} r_s \cdot \left(\frac{N^{ZH}}{N^s} \right) \cdot N_{ijk}^s - r_{bkg} \cdot N_{ijk}^{bkg} \right)^2}{N_{ijk}^{all}}, \quad (1)$$

where r_s represents the fitted parameters of r_{bb} , r_{cc} , r_{others} and r_{bkg} . N_{ijk}^s and N_{ijk}^{bkg} are the number of expected entries in each 3D sample bin (i, j, k), since each histogram is separated into n_b , n_c and n_{bc} bins. N_{ijk}^{data} are the number of simulated entries in each bin (i, j, k) by Toy-MC, which fluctuated with the Poisson distribution in each samples. In order to estimate the r_{bb} and r_{cc} , template fitting is applied with fluctuating the data by Poisson distribution and perform the 1,000 times Toy-MC analysis. Fitted r_{bb} and r_{cc}

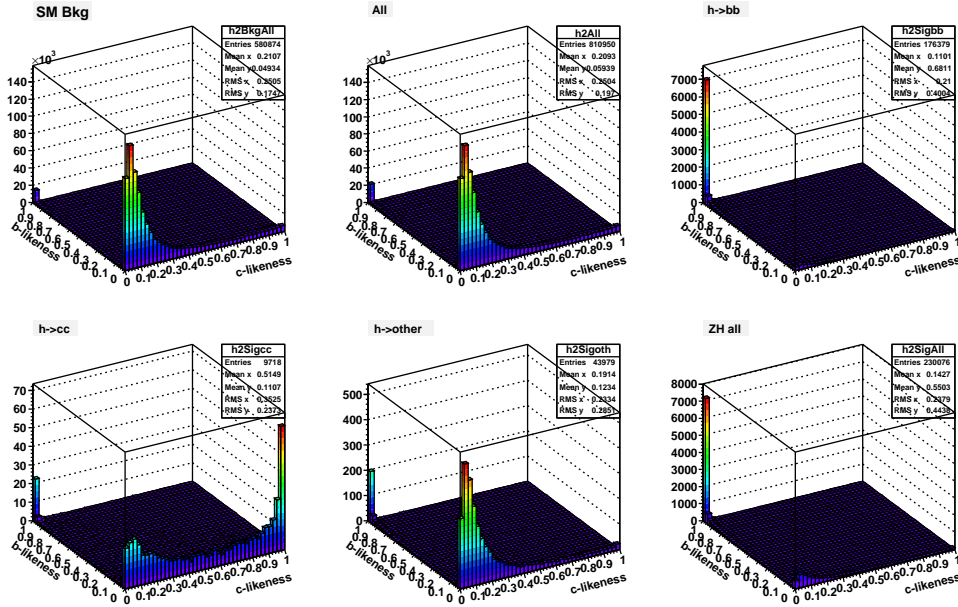


Figure 5: Image of the two-dimensional template sample histograms in b -likelihood and c -likelihood.

fractions are obtained from the distribution of the Toy-MC template fitted with Gaussian, as shown in Fig 6

From the 1,000 times Toy-MC template fitting, we obtain the r_{bb} and r_{cc} as 0.767 ± 0.002 , 0.422 ± 0.006 , which reproduce the true signal fractions of r_{bb} (0.765) and r_{cc} (0.0422), respectively.

From the limitation of the commonly reconstructed full simulation samples, especially for SM background, number of entries in each template sample 3D histogram, which depends on the histogram binning, become a systematic uncertainty of the fitted parameters. In order to reduce the histogram binning dependence, we apply the histogram smoothing for template samples. Fig. 7 shows the binning dependence after the smoothing.

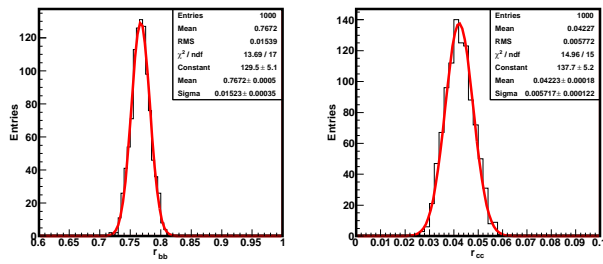


Figure 6: r_{bb} and r_{cc} distribution from the template fitting Toy-MC.

5 Results

The relative branching ratio in $H \rightarrow c\bar{c}$ to $H \rightarrow b\bar{b}$ is evaluated with following equation:

$$\frac{BR(H \rightarrow c\bar{c})}{BR(H \rightarrow b\bar{b})} = \frac{r_{cc}/\varepsilon_{cc}}{r_{bb}/\varepsilon_{bb}}, \quad (2)$$

where the $\varepsilon_{bb/cc}$ are the efficiency of $H \rightarrow b\bar{b}/c\bar{c}$ events after the selections as shown in Table 2. From the Eq. (2), relative branching fraction is obtained as:

$\frac{BR(H \rightarrow c\bar{c})}{BR(H \rightarrow b\bar{b})} = 0.058 \pm 0.008$, which corresponds to the measurement accuracy of 13.68%.

6 Conclusion

Measurement accuracy of Higgs branching ratio in Higgs hadronic decay mode $ZH \rightarrow q\bar{q}H$ in ILC experiment is evaluated at the $\sqrt{s} = 250$ GeV with assuming the Higgs mass of $M_H = 120$ GeV and the integrated luminosity of $\mathcal{L} = 250 \text{ fb}^{-1}$. From the template fitting analysis, measurement accuracy of the relative branching ratio of $H \rightarrow c\bar{c}$ to $H \rightarrow b\bar{b}$ is evaluated as 13.68%.

Acknowledgment

I would like to thank to everyone who join the ILC physics WG subgroup [10] for useful discussion of this work and to ILD optimization group members who maintain the software and MC samples.

References

- [1] ILC Reference Design Report (RDR) <http://www.linearcollider.org/rdr/>
- [2] J. Alcaraz [ALEPH Collaboration and CDF Collaboration and D0 Collaboration and an], arXiv:0911.2604 [hep-ex].
- [3] C. Anastasiou, G. Dissertori, M. Grazzini, F. Stockli and B. R. Webber, JHEP **0908**, 099 (2009) [arXiv:0905.3529 [hep-ph]].
- [4] GEANT4 Collaboration: S Agostinelli et al, Nucl. Instrum. Methods A506, 250 (2003).
- [5] <http://ilcsoft.desy.de/portal/>
- [6] <http://root.cern.ch/>
- [7] <http://acfahep.kek.jp/subg/sim/simtools/>
- [8] Nuclear Instruments and Methods in Physics Research Section A, Volume 610, Issue 2, p. 573-589.
- [9] T. Kuhl and K. Desch, LC-PHSM-2007-001
- [10] <http://www-jlc.kek.jp/subg/physics/ilcphys/>

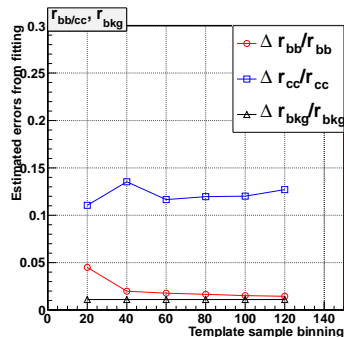


Figure 7: Binning dependence of the uncertainty of $r_{bb/cc}$ and r_{bkg} after the smoothing.